Supramolecular Chemistry

DOI: 10.1002/ange.201102370

Softening and Hardening of Macro- and Nano-Sized Organic Cocrystals in a Single-Crystal Transformation**

Chandana Karunatilaka, Dejan-Krešimir Bučar, Lindsay R. Ditzler, Tomislav Friščić, Dale C. Swenson, Leonard R. MacGillivray, and Alexei V. Tivanski**

The structure and properties of organic solids have great potential for rational design by using the principles of organic chemistry and supramolecular synthesis.[1–3] Understanding how to control the properties of organic solids, however, is a challenge owing to the sensitivity of close packing to subtle changes to molecular structure.[4,5] The reactivities of organic solids are of interest, especially those that undergo photoinduced single-crystal-to-single-crystal (SCSC) transformations.[6,7] Potential applications of solids that undergo SCSC reactions lie in pharmaceutical and materials science,[8–10] supramolecular synthesis,[11] and device applications, such as photoactivated molecular switches,[12,13] 3D data storage,[14–16] and nanoscale photomechanical actuators.[17] However, such promise is limited by a rarity of materials that undergo SCSC transformations. As photoirradiating a crystal will involve significant atomic motion, there is invariably an accumulation of stress and strain that causes crystals to crack and even crumble into a powder.[18]

Recent reports demonstrate that a SCSC reaction is possible in nanocrystals even when corresponding macrodimensional crystals do not display SCSC reactivity.[17,19,20] The possibility to induce SCSC reactions through miniaturizing crystals to nanodimensions can lead to the development of functional nanomaterials. The small size of nanocrystals can also result in physical and chemical properties that are different from macroscopic solids. The ability of nanocrystals to undergo photoinduced SCSC transformations can be attributed to a high surface-to-volume ratio that leads to more efficient stress and strain relaxation that is most likely absent for macrodimensional solids.[17] The exact nature of the relaxation is, however, unknown. Surprisingly, while a relaxation mechanism can be considered to be inherently related to the mechanical properties of a reactive solid, mechanical properties of solids that undergo SCSC transformations have not been investigated.[7] Mechanical properties also allow solid functionalities and allowable operating limits in device applications to be defined.[21] Moreover, gaining knowledge of mechanical properties of crystals that undergo SCSC transformations will thus, in addition to technological applications, be no doubt critical to develop an understanding of strain relaxation mechanisms and possibly allow the prediction of reactive properties.

Herein, we present a cocrystal[2,3] that undergoes a SCSC[6,7] transformation wherein the crystals undergo softening or hardening depending on size (Scheme 1). The components interact by hydrogen bonds and undergo an intermolecular [2+2] photodimerization.[11] Using atomic force microscopy (AFM) nanoindentation,[22–29] we show that unreacted cocrystals of millimeter dimensions are relatively soft and become 40% softer after photodimerization. We also show that the unreacted cocrystals undergo an 85% increase in stiffness upon being reduced to nanoscale dimensions and become 40% harder following the photoreaction. The changes in the mechanical properties are accompanied by a less than 0.1% change in density, which is attributed to the close spatial arrangement and minimal molecular movement that occurs during a SCSC transformation. Our findings provide a new perspective into understanding properties of organic solids that we believe can provide avenues to solids with unique mechanical and chemical properties.

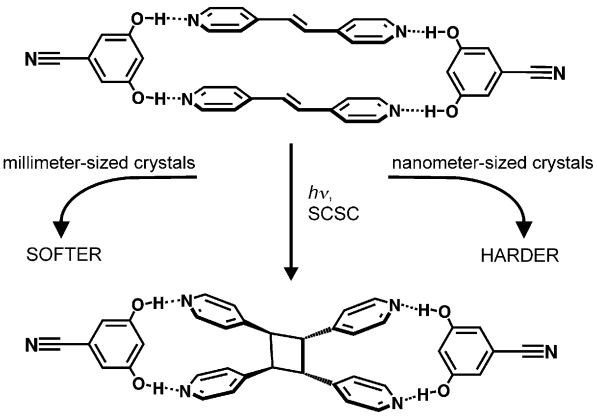

Scheme 1. Cocrystals of 2(5-CN-res)·2(4,4′-bpe), which undergo softening or hardening depending on crystal size. 5-CN-res = 5-cyanoresorcinol; 4,4′-bpe = *trans*-1,2-bis(4-pyridyl)ethylene.

AFM has been used to quantify changes in stiffness of single cocrystals of 2(5-CN-res)·2(4,4′-bpe) (where 5-CN-res = 5-cyanoresorcinol, 4,4′-bpe = *trans*-1,2-bis(4-pyridyl)-

[*] Dr. C. Karunatilaka,[+] D.-K. Bučar,[+] L. R. Ditzler, D. C. Swenson, Prof. Dr. L. R. MacGillivray, Prof. Dr. A. V. Tivanski
Department of Chemistry, University of Iowa
305 Chemistry Building, Iowa City, IA 52242 (USA)
E-mail: len-macgillivray@uiowa.edu
alexei-tivanski@uiowa.edu
Dr. T. Friščić
Department of Chemistry, University of Cambridge
Lensfield Road, Cambridge CB21EW (UK)
[+] These authors contributed equally to this work.

[**] C.K., L.R.D., and A.V.T. gratefully acknowledge financial support from the University of Iowa. D.K.B, T.F., and L.R.M acknowledge the National Science Foundation (DMR-0133138) for partial support.
Supporting information for this article is available on the WWW under http://dx.doi.org/10.1002/anie.201102370.

ethylene). The millimeter-sized crystals form through solvent evaporation, while nanococrystals form using reprecipitation combined with sonochemistry.[20] The cocrystal is composed of hydrogen-bonded assemblies wherein 5-CN-res preorganizes 4,4′-bpe for a [2+2] photodimerization. The reaction produces *rctt*-tetrakis(4-pyridyl)cyclobutane (4,4′-tpcb) in about 100% yield.[11]

A single-crystal X-ray diffraction study of millimeter-sized crystals of 2(5-CN-res)·2(4,4′-bpe) prior to UV irradiation demonstrates the components self-assemble by four O-H···N hydrogen bonds (O···N separations: 2.725(2), 2.728(2), 2.737(2), 2.744(2) Å; Figure 1). Powder X-ray diffraction (PXRD) confirmed the structure of the solid. As shown in Figure 1 a, 5-CN-res adopts a *syn*,*syn* conformation that enforces 4,4′-bpe into a face-to-face geometry such that the C=C bonds lie criss-crossed and separated by 3.82 Å.[4] The molecules pack in 2D layers in the crystallographic (010) plane, with the layers composed of stacks of 4,4′-bpe and the C≡N groups forming pairwise dipole–dipole interactions (C≡N separation: 3.41 Å). The C=C bonds of nearest-neighbor assemblies are separated by 4.03 Å. Upon exposure to UV radiation, 4,4′-bpe reacted to form 4,4′-tpcb in about 100% yield. Importantly, optical microscopy revealed the crystals to retain transparency and general morphology during the photoreaction, which suggested the crystals underwent a SCSC transformation.[6,7] An X-ray analysis confirmed a SCSC transformation (Table 1), with the C=C bonds reacting in each assembly[30] and the hydrogen bonds being maintained (O···N separations: 2.675(2), 2.699(3), 2.724(3), 2.737(3) Å; Figure 1 a).

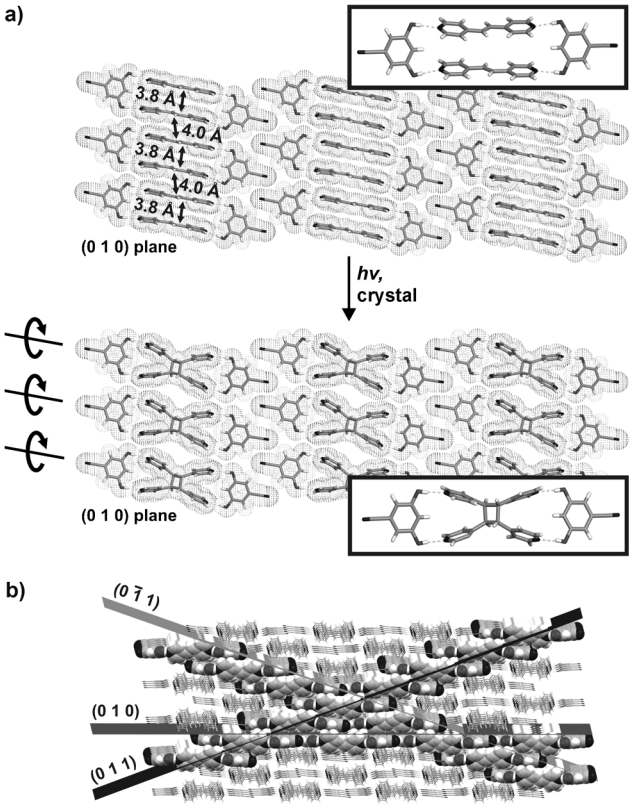

Figure 1. SCSC reactivity of 2(5-CN-res)·2(4,4′-bpe) to form 2(5-CN-res)·2(4,4′-tpcb): a) layers of the (010) crystallographic plane and b) crystallographic planes (010), (011), and (0−11).

Table 1: X-ray crystallographic data and Young's moduli for unreacted and reacted cocrystals of 2(5-CN-res)·2(4,4′-bpe).

	Unreacted	Photoreacted
Crystallographic data:		
space group	$P\bar{1}$	$P\bar{1}$
a [Å]	7.6903(9)	7.7709(9)
b [Å]	9.4154(11)	9.8124(11)
c [Å]	24.120(3)	23.620(3)
α [°]	86.888(5)	86.635(5)
β [°]	89.295(5)	89.850(5)
γ [°]	71.235(5)	66.617(5)
V [Å^3]	1651.2(3)	1649.9(3)
ρ_{calc} [g cm^{-3}]	1.277	1.278
T [K]	298(2)	298(2)
AFM nanoindentation:[a]		
millimeter-sized, (011)	(260±20)/120	(150±12)/75
millimeter-sized, (0−11)	(240±28)/100	(150±11)/125
nanometer-sized	(460±40)/90	(635±70)/110

[a] Stiffness [MPa]/no. of different crystal positions for Young's modulus measurements.

A comparison of the unit cell dimensions showed that the cell undergoes a significant change in the SCSC reaction. Whereas the volume and density remained virtually unchanged, the *γ* angle decreased from 71.2° to 66.6° (Table 1). The decrease corresponds to an orientational tilt of each 5-CN-res molecule along the C≡N axis (angles: 3.3° and 4.9°; Figure 1 a). The tilt accommodates the generation of 4,4′-tpcb whilst maintaining the dipole–dipole forces (C≡N separation: 3.43 Å). The physical stress that the crystal experienced during the reaction was thus most likely absorbed by movements of the components to retain single-crystal character.

That 2(5-CN-res)·2(4,4′-bpe) underwent a SCSC transformation prompted us to investigate mechanical properties using AFM nanoindentation. Whereas AFM has been used to measure changes in elastic behavior of chemical cross-links in polymers[25] and thin films,[26] as well as morphological changes of reactive single crystals,[31] we are unaware of an example wherein AFM nanoindentation has been used to study mechanical properties of a SCSC transformation.

Our first studies involved the millimeter-sized crystals. The crystals exhibited prism morphologies with a base of approximately 0.40 mm × 0.60 mm and height 0.10 mm. Top and bottom crystal faces that correspond to the crystallographic (011) and (0−11) planes (Figure 1 b) were characterized by AFM. Each plane lies parallel to the crystallographic *a* axis and at 20° to the 2D layers. Both planes are chemically similar, being composed of 5-CN-res and 4,4′-bpe molecules that interact by hydrogen bonds and edge-to-face π–π forces.

As shown in Figure 2 a,b, our AFM studies revealed the (011) and (0−11) faces to exhibit distinct topographies. The (011) face was composed of terraces and small spiral pyramids with a typical base size and height of 1 μm and 20 nm, respectively. Measurements of the height of the pyramid step

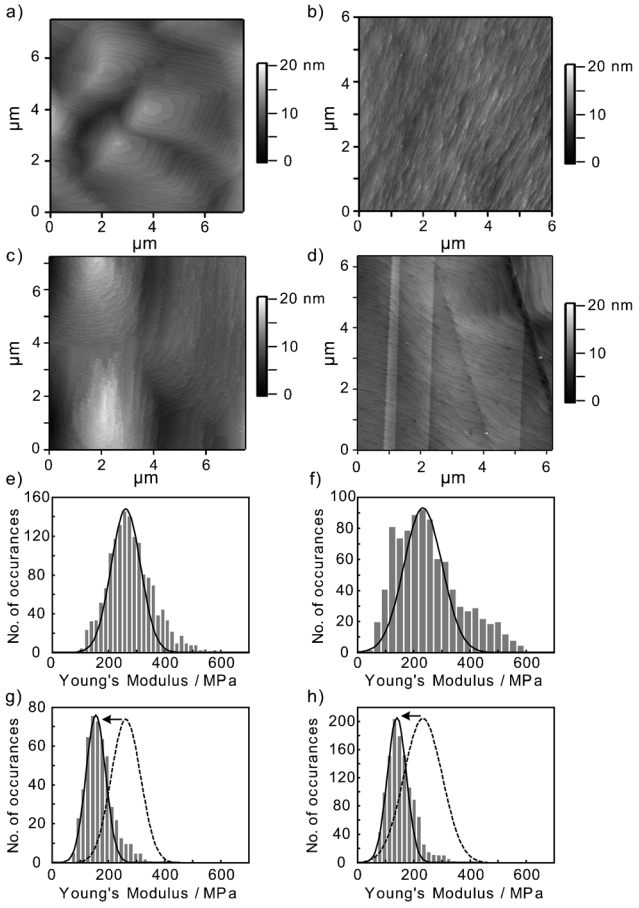

Figure 2. AFM height images and histograms of the Young's modulus values for millimeter-sized 2(5-CN-res)·2(4,4′-bpe). a) Unreacted (011) face, showing terraces and spiral pyramids and b) unreacted (0−11) face, showing uniform layer-type morphology. c,d) Photoreacted (011) (c) and (0−11) (d) surfaces of same crystal show the morphology remained largely intact. e,g) Young's modulus distributions of the (011) face before (e) and after (g) photoreaction, showing 42% decrease in stiffness. f,h) Young's modulus distributions of the (0−11) face before (f) and after (h) photoreaction, showing a 38% decrease in stiffness. Black lines shown in (e–h) are the Gaussian fits. Dotted lines in (g) and (h) are Gaussian fits for the corresponding faces of unreacted crystals. Arrows indicate directional changes in stiffness.

and the normal terrace revealed a constant height of approximately 7 Å. The height corresponds to edge-to-face π–π interactions (ca. 7 Å) involving 5-CN-res and 4,4′-bpe. In contrast, the (0−11) face displayed a uniform and nearly-flat morphology. The fundamental unit of crystal growth can thus be considered to be propagated by the π–π interactions, with growth beginning along the flat (0−11) face and ending with the spiral pyramids of the (011) face. The pyramids most likely form at the conclusion of the crystal growth process.[32]

AFM height images obtained for the millimeter-sized crystals after photoreaction are shown in Figure 2c,d. Both morphologies remained intact, although slight irregularities as rough edges and granular sub-nanometer features appeared on the outer terrace regions. The cleavage planes showed for the (011) surface were also observed for unreacted crystals and thus do not necessarily form as a result of the reaction. The nominal changes in the morphologies are consistent with the SCSC transformation.

Mechanical measurements were then performed on the millimeter-sized crystals both before and after photoreaction using AFM nanoindentation.[22–29] Repeated force–displacement curves were recorded at approximately 100 crystal positions to determine the local stiffness, or Young's modulus. The Young's moduli determined for all crystal positions were combined, and histograms from three different crystals are shown in Figure 2e–h and summarized in Table 1. The elasticity measurements yielded an average Young's modulus (mean ± s.d.) for the (011) face of (260 ± 20) MPa before photoreaction (Figure 2e) that decreased to (150 ± 12) MPa (42% change) after photoreaction (Figure 2g). The (0−11) face similarly showed a decrease in crystal stiffness with the Young's modulus values of (240 ± 28) MPa and (150 ± 11) MPa (38% change), respectively (Figure 2f,h). The widths of both Young's moduli distributions also narrowed relative to unreacted responses. The resulting values are comparable to protein crystals (165 MPa),[29] hyperbranched macromolecules (190 MPa),[27] and low-density polyethylene (100 MPa),[33] but up to 25 times softer than crystalline acetaminophen (8.4 GPa),[34] high-density polyethylene (7.5 GPa),[33] and aspirin (7.1 GPa).[35]

Two important conclusions can be drawn from the AFM data. First, the crystals clearly become less stiff following the SCSC transformation. Second, the extent of softening is similar for the (011) and (0−11) faces, with an average decrease in stiffness of approximately 40%. An identical response is expected given that the faces are chemically similar. The changes in the mechanical properties after photoreaction are especially noteworthy, as the change in crystal density is less than 0.1% (Table 1).[36]

To gain further insight into the decrease in stiffness, cocrystals of 2(5-CN-res)·(4,4′-tpcb) were independently prepared from solution. In contrast to the SCSC reaction, the components of the as-synthesized solid formed a 1D hydrogen-bonded polymer wherein 5-CN-res adopts a *syn*,-*anti* conformation (see Supporting Information). The solid is thus a polymorph of the product of the SCSC reaction.[37] The formation of the polymorph supports the product of the SCSC reaction being metastable, which may account for the decrease in stiffness following photoreaction. Mechanical measurements on the (101) face of the polymorph, however, yielded an average Young's modulus of (105 ± 10) MPa. As the polymorph most likely has fewer defects than the product of the SCSC reaction, the softening can also be attributed to the photochemically induced change in composition of the components.

The nanometer-sized solid was then studied. As crystal planes at a surface can relax more easily at the nanoscale,[28] the nanocrystals were expected to involve more efficient strain relaxation. SEM micrographs and representative AFM 3D height images were collected for the nanococrystals before and after reaction (Figure 3a–d). The images revealed prisms with a base size distribution from 150 nm to 1 µm and a typical height of 100 nm. XRPD data confirmed the structure as photoactive 2(5-CN-res)·2(4,4′-bpe). Exposure of the nanococrystals to UV radiation afforded 4,4′-tpcb, while

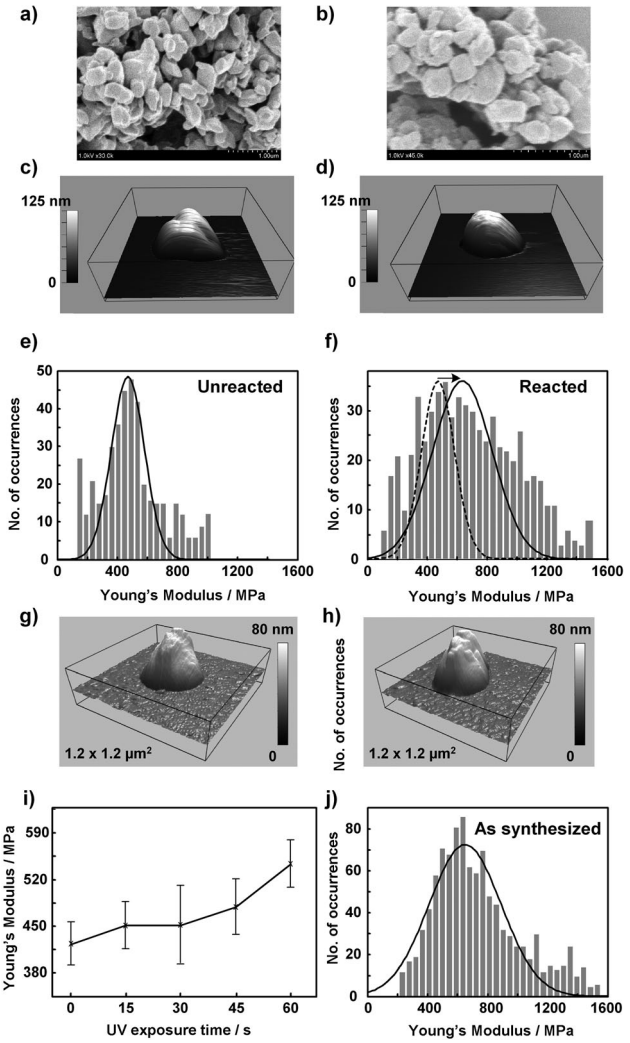

Figure 3. SEM and AFM images and Young's modulus values for 2(5-CN-res)·2(4,4′-bpe) nanococrystals. a,b) Unreacted and reacted nanococrystals with prism-like shapes. c,d) Unreacted and reacted AFM height images (1 µm × 1 µm) of two nanococrystals having approximately the same height. e,f) Young's modulus values before (e) and after (f) photoreaction, showing 40% increase in stiffness. g–i) In situ AFM measurements: AFM height image of nanocrystal before (g) and after (h) UV exposure for 60 s; i) increase in the averaged Young's modulus of the nanocrystal versus UV exposure time. j) Young's modulus of as-synthesized nanocrystals of 2(5-CN-res)·(4,4′-tpcb).

SEM micrographs demonstrated that the crystals maintain integrity following photoreaction, which was confirmed by XRPD analysis.

Mechanical measurements were then performed on individual nanococrystals before and after the photoreaction. Histograms of the Young's modulus values are shown in Figure 3e,f, respectively. The AFM measurements yielded average Young's modulus values (mean ± s.d.) of (460 ± 40) MPa for the unreacted nanocrystals that increased to (635 ± 70) MPa after the photoreaction. We note that it was not possible to determine crystallographic faces of the nanocrystals probed using the AFM tip and thus the modulus values represent an ensemble-averaged response.[28] Nevertheless, the decrease in the cocrystal dimensions from millimeter to nanometer-size resulted in an increase of the Young's modulus from 250 MPa to 460 MPa, or an 85% increase in crystal stiffness. The nanometer-sized cocrystals also became 40% stiffer, or harder, following the photoreaction. The overall stiffening of the nanococrystals is in sharp contrast with the millimeter-sized crystals, where an opposite effect was observed. Related size effects have been reported for a thin film with dimensions less than several hundred nanometers,[28] where size dependences were attributed to an increase in the surface-to-volume ratio.

The mechanical response of an individual nanococrystal was also measured in situ using AFM nanoindentation. The measurements determined the average Young's modulus before photoreaction to be (435 ± 35) MPa. Exposures to UV light (365 nm) were achieved using an objective located below a UV transparent quartz slide, which allowed the AFM measurements to be performed in real time during the photodimerization. Four sequential 15 s UV exposures were applied, and after each exposure the nanococrystal was reimaged and the Young's modulus was determined (Figure 3g–i) Whereas the crystal remained intact with no apparent changes to crystal size, a steady increase in the Young's modulus up to 30% was observed, which is consistent with the ensemble-average response (40%). The result unambiguously supports the proposal of the nanococrystals becoming harder after photoreaction.

Nanoindentation was also performed on an as-synthesized sample of 2(5-CN-res)·(4,4′-tpcb) prepared by sonochemistry (Figure 3j). The preparation afforded nanococrystals with a structure (as seen from PXRD) that is different than the polymorph, yet similar to the product of the SCSC reaction. The distribution yielded an average modulus value of (650 ± 90) MPa, which agrees well with the SCSC transformation (ca 635 MPa).

In conclusion, AFM nanoindentation has been used to study mechanical properties of millimeter- and nanometer-sized crystals that undergo a SCSC photodimerization. Crystals of millimeter dimensions become 40% softer, while crystals of nanoscale dimensions become 40% harder following photoreaction. The changes are accompanied by a less than 0.1% change in density. The decrease in crystal size from millimeters to nanometers led to an 85% increase in crystal stiffness. We expect our findings to open possibilities to crystal engineer[1] materials with unique mechanical properties.

Experimental Section

Millimeter crystals of 2(5-CN-res)·2(4,4′-bpe) were grown by slow solvent evaporation. 4,4′-bpe (0.182 mg, 1 mmol) and 5-CN-res (135 mg, 1 mmol) were dissolved separately in dry acetonitrile (99.9%; 5 mL total). The solutions were combined and filtered through a Millex syringe filter (PVDF, 0.2 µm, 13 mm). The solution was left to evaporate over 5 days to afford crystals for single-crystal X-ray diffraction. The nanococrystals were obtained by precipitation combined with sonochemistry. Solutions were filtered through a Millex syringe filter (PVDF, 0.2 µm, 13 mm) directly into cool hexanes (ca. 0 °C, 225 mL) while exposed to low-intensity ultrasonic radiation (ultrasonic cleaning bath Branson 2510R-DTM, frequency:

42 kHz, 6% at 100 W). The resulting suspension was sonicated for 1–2 min, filtered, and dried at room temperature.

Nanometer-sized crystalline samples were suspended in hexanes at 0.25 mg mL^{-1} and then deposited on a freshly cleaved atomically flat mica substrate (*V–I* grade, SPI Supplies, Westchester, PA). Millimeter-sized crystals were directly placed on a clean glass cover slip. All AFM studies were conducted using a molecular force probe 3D AFM (Asylum Research, Santa Barbara, CA). AFM height images and nanoindentation measurements were collected at room temperature using silicon probes (MikroMasch, San Jose, CA, CSC37) with a nominal spring constant of 0.35 N m^{-1} and a typical tip radius of curvature of 10 nm. Force–displacement curves were recorded in an organic solvent (*n*-tetradecane, Fluka) using a total of 16 AFM probes. The force curves data were used to estimate the Young's modulus of a crystal by using a rearranged form of the Hertzian model.[28,29,38–42] The substrate-induced effects on the measured Young's modulus values were negligible here as the height of a nanocrystal (ranging from 50 to 400 nm) is more than one order of magnitude larger than typical indentation depth of 3.5 nm.

Diffraction data were measured on a Nonius Kappa CCD single-crystal X-ray diffractometer at room temperature (25 °C) using MoK_α radiation ($\lambda = 0.71073$ Å). Structure solution and refinement were accomplished using SHELXS-97 and SHELXL-97, respectively.[43] All non-hydrogen atoms were refined anisotropically. Hydrogen atoms associated with carbon atoms were refined in geometrically constrained positions. Hydrogen atoms associated with oxygen atoms were calculated in an optimal hydrogen bonding geometry.

XRPD data were obtained on a Siemens D5000 X-ray diffractometer using Cu$K_{\alpha 1}$ radiation ($\lambda = 1.54056$ Å) (scan type: locked coupled; scan mode: continuous; step size: 0.02°; scan time: 2 s/step).

CCDC 773873 (unreacted) and CCDC 773874 (reacted) contain the supplementary crystallographic data for this paper. These data can be obtained free of charge from The Cambridge Crystallographic Data Centre via www.ccdc.cam.ac.uk/data_request/cif.

Received: April 6, 2011
Published online: July 20, 2011

Keywords: atomic force microscopy · nanomaterials · self-assembly · single-crystal transformations · supramolecular chemistry

[1] G. R. Desiraju, *Angew. Chem.* **1995**, *107*, 2541 – 2558; *Angew. Chem. Int. Ed. Engl.* **1995**, *34*, 2311 – 2327.
[2] G. P. Stahly, *Cryst. Growth Des.* **2009**, *9*, 4212 – 4229.
[3] T. Friščić, W. Jones, *Cryst. Growth Des.* **2009**, *9*, 1621 – 1637.
[4] G. M. J. Schmidt, *Pure Appl. Chem.* **1971**, *27*, 647 – 678.
[5] J. J. Wolff, *Angew. Chem.* **1996**, *108*, 2339 – 2341; *Angew. Chem. Int. Ed. Engl.* **1996**, *35*, 2195 – 2197.
[6] T. Friščić, L. R. MacGillivray, *Z. Kristallogr.* **2005**, *220*, 351 – 363.
[7] I. Halasz, *Cryst. Growth Des.* **2010**, *10*, 2817 – 2823.
[8] N. Shan, M. J. Zaworotko, *Drug Discovery Today* **2008**, *13*, 440 – 446.
[9] M. Morimoto, S. Kobatake, M. Irie, *Chem. Commun.* **2008**, 335 – 337.
[10] A. N. Sokolov, T. Friščić, L. R. MacGillivray, *J. Am. Chem. Soc.* **2006**, *128*, 2806 – 2807.
[11] L. R. MacGillivray, G. S. Papaefstathiou, T. Friščić, T. D. Hamilton, D.-K. Bučar, Q. Chu, D. B. Varshney, I. G. Georgiev, *Acc. Chem. Res.* **2008**, *41*, 280 – 291.
[12] B. L. Feringa, R. A. van Delden, N. Koumura, E. M. Geertsema, *Chem. Rev.* **2000**, *100*, 1789 – 1816.
[13] M. Irie, *Chem. Rev.* **2000**, *100*, 1685 – 1716.
[14] M. A. Garcia-Garibay, *Angew. Chem.* **2007**, *119*, 9103 – 9105; *Angew. Chem. Int. Ed.* **2007**, *46*, 8945 – 8947.
[15] S. Kawata, Y. Kawata, *Chem. Rev.* **2000**, *100*, 1777 – 1788.
[16] F. Li, J. Zhuang, G. Jiang, H. Tang, A. Xia, L. Jiang, Y. Song, Y. Li, D. Zhu, *Chem. Mater.* **2008**, *20*, 1194 – 1196.
[17] R. O. Al-Kaysi, A. M. Müller, C. J. Bardeen, *J. Am. Chem. Soc.* **2006**, *128*, 15938 – 15939.
[18] I. Turowska-Tyrk, *J. Phys. Org. Chem.* **2004**, *17*, 837 – 847.
[19] S. Takahashi, H. Miura, H. Kasai, S. Okada, H. Oikawa, H. Nakanishi, *J. Am. Chem. Soc.* **2002**, *124*, 10944 – 10945.
[20] D.-K. Bučar, L. R. MacGillivray, *J. Am. Chem. Soc.* **2007**, *129*, 32 – 33.
[21] C. M. Reddy, G. R. Krishna, S. Ghosh, *CrystEngComm* **2010**, *12*, 2296 – 2314.
[22] R. F. Cook, *Science* **2010**, *328*, 183 – 184.
[23] O. Sahin, S. Magonov, C. Su, C. F. Quate, O. Solgaard, *Nat. Nanotechnol.* **2007**, *2*, 507 – 514.
[24] D. Tranchida, Z. Kiflie, S. Acierno, S. Piccarolo, *Meas. Sci. Technol.* **2009**, *20*, 095702.
[25] E. Wornyo, K. Gall, F. Yang, W. King, *Polymer* **2007**, *48*, 3213 – 3225.
[26] J. Domke, M. Radmacher, *Langmuir* **1998**, *14*, 3320 – 3325.
[27] H. Shulha, X. Zhai, V. V. Tsukruk, *Macromolecules* **2003**, *36*, 2825 – 2831.
[28] a) J.-G. Guo, Y.-P. Zhao, *J. Appl. Phys.* **2005**, *98*, 074306; b) J. R. G. Sander, D.-K. Bučar, R. F. Henry, G. G. Z. Zhang, L. R. MacGillivray, *Angew. Chem.* **2010**, *122*, 7442 – 7446; *Angew. Chem. Int. Ed.* **2010**, *49*, 7284 – 7288.
[29] S. Guo, B. B. Akhremitchev, *Langmuir* **2008**, *24*, 880 – 887.
[30] Q. Chu, D. C. Swenson, L. R. MacGillivray, *Angew. Chem.* **2005**, *117*, 3635 – 3638; *Angew. Chem. Int. Ed.* **2005**, *44*, 3569 – 3572.
[31] a) G. Kaupp, *Angew. Chem.* **1992**, *104*, 609 – 612; *Angew. Chem. Int. Ed. Engl.* **1992**, *31*, 595 – 598; b) G. Kaupp, *Angew. Chem.* **1992**, *104*, 606 – 609; *Angew. Chem. Int. Ed. Engl.* **1992**, *31*, 592 – 595.
[32] S. Dumrul, S. Bazzana, J. Warzywoda, R. R. Biederman, A. Sacco, *Microporous Mesoporous Mater.* **2002**, *54*, 79 – 88.
[33] M. S. Bischel, M. R. Vanlandingham, R. F. Eduljee, J. W. Gillespie, J. M. Schultz, *J. Mater. Sci.* **2000**, *35*, 221 – 228.
[34] W. C. Duncan-Hewitt, G. C. Weatherly, *J. Mater. Sci. Lett.* **1989**, *8*, 1350 – 1352.
[35] R. J. Roberts, R. C. Rowe, P. York, *Powder Technol.* **1991**, *65*, 139 – 146.
[36] Cross-linking of polymers typically leads to an increase in stiffness accompanied by an increase in density. For examples, see: a) T. Boudou, T. Crouzier, R. Auzély-Velty, K. Glinel, C. Picart, *Langmuir* **2009**, *25*, 13809 – 13819; b) H. Dal, M. Kaliske, *PAMM* **2006**, *6*, 363 – 364; c) S. M. Kurtz, L. A. Pruitt, C. W. Jewett, J. R. Foulds, A. A. Edidin, *Biomaterials* **1999**, *20*, 1449 – 1462.
[37] For a polymorph, see: G. Novak, V. Enkelmann, G. Wegner, K. B. Wagener, *Angew. Chem.* **1993**, *105*, 1678 – 1680; *Angew. Chem. Int. Ed. Engl.* **1993**, *32*, 1614 – 1616.
[38] J. L. Hutter, J. Bechhoefer, *Rev. Sci. Instrum.* **1993**, *64*, 1868 – 1873.
[39] N. A. Burnham, R. J. Colton, *J. Vac. Sci. Technol. A* **1989**, *7*, 2906 – 2913.
[40] H. J. Hertz, *Reine Angew. Math.* **1881**, *92*, 156 – 171.
[41] L. R. Ditzler, C. Karunatilaka, V. R. Donuru, H. Y. Liu, A. V. Tivanski, *J. Phys. Chem. C* **2010**, *114*, 4429 – 4435.
[42] K. Bowmen, *Mechanical Behavior of Materials*, 1. ed., Wiley, Hoboken, NJ, **2004**.
[43] G. M. Sheldrick, *Acta Crystallogr. Sect. A* **2008**, *64*, 112 – 122.

